REPRODUCTION
RESEARCH

Mitochondrial humanin peptide acts as a cytoprotective factor in granulosa cell survival

Carolina Marvaldi[1,2], Daniel Martin[1,3], Julia G Conte[1], María Florencia Gottardo[1,4], Matías L Pidre[5], Mercedes Imsen[1], Martin Irizarri[1,3], Sharron L Manuel[6], Francesca E Duncan[6], Víctor Romanowski[5], Adriana Seilicovich[1,3] and Gabriela Jaita[1,3]

[1]Instituto de Investigaciones Biomédicas (INBIOMED) UBA-CONICET, Facultad de Medicina, Uiversidad de Buenos Aires, Buenos Aires, Argentina, [2]Laboratorio de Fisiopatología de la Preñez y el Parto, Centro de Estudios Farmacológicos y Botánicos (CEFyBO) UBA-CONICET, Facultad de Medicina, Universidad de Buenos Aires, Buenos Aires, Argentina, [3]Departamento de Biología Celular e Histología, Facultad de Medicina, Universidad de Buenos Aires, Buenos Aires, Argentina, [4]Laboratorio de Oncología Molecular, Universidad Nacional de Quilmes, Buenos Aires, Argentina, [5]Instituto de Biotecnología y Biología Molecular (IBBM), Universidad Nacional de La Plata – CONICET, La Plata, Argentina and [6]Department of Obstetrics and Gynecology, Feinberg School of Medicine, Northwestern University, Chicago, Illinois, USA

Correspondence should be addressed to G Jaita; Email: gjaita@fmed.uba.ar

Abstract

Humanin (HN) is a short peptide involved in many biological processes such as apoptosis, cell survival, inflammatory response, and reaction to stressors like oxidative stress, between others. In the ovary, a correct balance between pro- and anti-apoptotic factors is crucial for folliculogenesis. In the follicular atresia, survival or death of granulosa cells is a critical process. The goal of this study was to evaluate the action of HN on granulosa cell fate. To explore endogenous HN function in the ovary, we used a recombinant baculovirus (BV) encoding a short-hairpin RNA targeted to silence HN (shHN). HN downregulation modified ovarian histoarchitecture and increased apoptosis of granulosa cells. HN was also detected in a granulosa tumor cell line (KGN). Transduction of KGN cells with BV-shHN resulted in HN downregulation and increased apoptosis. On the other hand, treatment of KGN cells with exogenous HN increased cell viability and decreased apoptosis. In summary, these findings indicate that HN is a cytoprotective factor in granulosa cells of antral follicles, suggesting that this peptide would be involved in the regulation of folliculogenesis. Also, this peptide is a cytoprotective factor in KGN cells, and therefore, it could be involved in granulosa tumor cell behavior.

Reproduction (2021) **161** 581–591

Introduction

Humanin (HN) is a 24 amino acid peptide that was originally identified as an anti-apoptotic peptide in healthy neurons of a patient with Alzheimer's disease (Hashimoto *et al.* 2001*a*). The homologous rat gene encodes a 38 amino acid peptide (Caricasole *et al.* 2002). Both peptides share amino acid residues essential for homodimerization, secretion and neuroprotection (Hashimoto *et al.* 2004, Nishimoto *et al.* 2004, Zapała *et al.* 2010, Zuccato *et al.* 2018). HN peptides were reported to be encoded in mitochondrial DNA within the 16S rRNA coding region (Paharkova *et al.* 2015).

HN peptides were detected in several tissues including cerebral cortex, hippocampus, heart, skeletal muscle, plasma, pituitary, testicles, and uterus (Hashimoto *et al.* 2001*a*,*b*, Caricasole *et al.* 2002, Yadav *et al.* 2004, Kariya *et al.* 2005, Moretti *et al.* 2010, Widmer *et al.* 2013, Gottardo *et al.* 2015). In reproductive tissues such as testicles, HN is expressed in Leydig cells (Colón *et al.* 2006) as well as in vessels, spermatocytes and sperm (Moretti *et al.* 2010). HN is located in the mid-piece of normal sperm and in cytoplasmic residues of abnormal sperm, so HN localization has been proposed to be a marker of sperm quality and motility (Moretti *et al.* 2010, Rao *et al.* 2018). Leydig cells can release HN *in vitro* which promotes cell survival, acting as an autocrine factor, and enhancing the steroidogenesis rate (Colón *et al.* 2006). Testicular hormone deprivation and excess of insulin-like growth factor-binding protein-3 (IGFBP3) induce apoptosis of germ cells of rat and mouse testicles, the effect that is attenuated by HN administration (Lue *et al.* 2010). These studies suggest that HN has an important function in the cytoprotection of testicular cells and, therefore, in the regulation of spermatogenesis (Lue *et al.* 2010). In the ovary, the absence of gonadotropins increases the transcriptional expression of HN in the corpus luteum (Yadav *et al.* 2004).

© 2021 Society for Reproduction and Fertility
ISSN 1470–1626 (paper) 1741–7899 (online)
https://doi.org/10.1530/REP-20-0197
Online version via https://rep.bioscientifica.com
Downloaded from Bioscientifica.com at 11/28/2022 10:27:47AM
via free access

Recently, it has been shown that HN is present in the human ovary and follicular fluid (Rao *et al.* 2018). However, the localization and action of HN in the ovary along folliculogenesis have not been elucidated yet.

In the ovary, regulation of apoptosis plays an important role in the maintenance of follicular development, and thus, in ovarian function in each menstrual cycle (Tilly *et al.* 1995). During folliculogenesis, primordial follicles mature and increase their size until they reach the antral follicle stage. These follicles are composed of two different cell types: granulosa cells, which produce estradiol and follicular fluid (Rodgers & Irving-Rodgers 2010), and theca cells, which act as a structural support and produce androgenic precursors (Young & McNeilly 2010). Before reaching the preovulatory stage, most follicles are eliminated by the degenerative process of atresia. This phenomenon occurs mainly by the apoptosis of granulosa cells (Hsueh *et al.* 1994). Follicular development is essential in female reproduction, and dysfunctional folliculogenesis could lead to several pathologies such as polycystic ovary syndrome (PCOS), premature ovarian aging and infertility (Lim & Luderer 2011, Agarwal *et al.* 2012, Lim *et al.* 2015).

The aim of the present study was to evaluate the localization and action of HN peptides in rat ovary and in a human granulosa tumor cell line (KGN). To analyze the role of endogenous HN in the ovary and KGN cells, we studied the effect of downregulation of endogenous HN on the histoarchitecture and apoptosis in adult rat ovary and on KGN cell survival. To this end, we used a baculovirus (BV) encoding a short-hairpin RNA (shRNA) targeted to HN mRNA (Gottardo *et al.* 2018). We also investigated the action of exogenous HN on KGN cells, using a synthetic HN peptide. Our results indicate that HN acts as a pro-survival factor in normal and tumor granulosa cells.

Materials and methods

Ethics statement

All procedures in this study were approved by the Ethics Committee of the School of Medicine, University of Buenos Aires (Res. No 1727/2017) and were performed in accordance with the standards of the National Institutes of Health (NIH), as described in the guide for Care and Use of Laboratory Animals.

Drugs

All chemicals were purchased from Sigma Chemical Co. except those indicated in the following paragraphs. Sources for reagents used in specific procedures are included in the description of the particular method.

Animals

Adult (2–3 months) and prepubertal Wistar rats (21–23 days) were kept under controlled conditions of temperature (21–22°C) and 12 h light:12 h darkness cycle with free access to food and water. Rats were monitored by daily vaginal smears over three consecutive cycles and euthanized in proestrus or diestrus. To obtain ovaries enriched with follicles at different developmental stages, prepubertal rats were injected s.c. either with diethylstilbestrol (DES 1 mg/rat), dissolved in corn oil, daily, for 3 days, to stimulate the development of early antral follicles (EAF) or with a single injection of equine chorionic gonadotropin (PMSG, 25 IU/rat, Novormon, Syntex S.A. Buenos Aires, Argentina) 48 h before the experiment, to stimulate the development of preovulatory follicles (POF) (Li *et al.* 1998). To downregulate HN expression *in vivo*, another group of adult rats was anesthetized with ketamine (75 mg/kg, i.p.) and xylazine (5 mg/kg, i.p.), the ovaries were exteriorized through an incision made in the dorsolumbar region. Rats were injected under the bursa of one ovary with 10^7 viral particles of BV-shHN (10 µL/ovary). The contralateral ovary was injected with 10^7 viral particles of BV-control used as a control. An additional control was designed in which one ovary was injected with BV-control and the contralateral with PBS (resuspension buffer of BV). No significant differences were found between these two treatments. Therefore, BV-control was used as control in the following experiments. After injection, ovaries were replaced, the incision was closed and rats were treated with ketoprofen (5 mg/kg) for analgesia. Rats were euthanized 14 days after surgery.

Ovarian morphology

The ovaries were removed and immediately frozen in liquid nitrogen or fixed in 4% paraformaldehyde (PFA) for 4 h, dehydrated in a graded series of ethanol and embedded in paraffin. To prevent counting the same follicle twice, 5 µm step sections were mounted at 50 µm intervals onto microscope slides according to the method previously described (Woodruff *et al.* 1990). One set of slides was stained with hematoxylin and eosin and another was used to detect apoptotic cells by TUNEL, immunolocalization of HN or Picrosirius Red staining. Follicles were classified as either normal or atretic. Atretic follicle was defined as that characterized by degeneration and detachment of granulosa cell layer from the basement membrane and the presence of more than 10 pyknotic nuclei and degenerate oocytes (Parborell *et al.* 2008).

Immunolocalization of HN

The presence of HN in ovarian sections and KGN cells was evaluated by indirect immunofluorescence or immunohistochemistry staining. Ovarian sections (5 µm) were deparaffinized in xylene and rehydrated in a series of graded ethanol bath (100, 96, 90, 70%). Tissue sections were incubated with anti-HN antibody (Sigma, 1:100) overnight and revealed with peroxidase-conjugated anti-rabbit IgG (Vector Laboratories, 1:200) and hematoxylin counterstained. The appearance of a brown reaction product was observed by light microscope. KGN cells were seeded on glass coverslips and fixed in 4% PFA. Cells were incubated for 1 h with anti-HN antibody (Sigma 1:100), washed and incubated for 1 h with anti-rabbit FITC (Vector Laboratories, 1:200). Finally,

Downloaded from Bioscientifica.com at 11/28/2022 10:27:47AM
via free access

slides were mounted with mounting medium for fluorescence (Vectashield, Vector Laboratories) containing DAPI. Cells were visualized using a fluorescence light microscope (Axiophot, Carl Zeiss). Nonspecific control was incubated with nonspecific IgG instead of the anti-HN-specific primary antibody.

Picrosirius red staining

Fibrosis is due to an increase in collagen I and III and has been shown to occur in the ovary with age (Briley *et al.* 2016). To determine collagen content within rat ovarian tissue, we followed a previously described staining protocol (Briley *et al.* 2016) using picrosirius red (PSR), a highly-specific histological dye for collagen I and III fibers. Tissue sections were deparaffinized in Citrisolv (Fisher Scientific) and then rehydrated in a series of graded ethanol baths (100, 70 and 30%). Slides were then immersed in a PSR staining solution prepared by dissolving Sirius Red F3BA (Direct Red 80) in a 1.3% saturated aqueous solution of picric acid at 0.1% (w/v). Slides were incubated in the PSR staining solution for 40 min at room temperature. The slides were then washed in acidified water consisting of 0.05 M hydrochloric acid (Fisher Scientific) for 90 s. Excess acidified water was carefully wicked away from the tissue sections, and the tissue was rapidly dehydrated in 100% ethanol (a total of three, 30 s incubations). The slides were cleared in Citrisolv for 5 min and mounted with Cytoseal XYL (Fisher Scientific). Whole ovary sections were imaged by brightfield microscopy on the EVOS FL Auto system at 10× magnification using the scanning function. The brightness, contrast and saturation were set to the default settings of the instrument and remained consistent throughout imaging of all PSR-stained sections.

To quantify the area of ovarian tissue that was positive for PSR staining we followed the protocol as described (Briley *et al.* 2016). Briefly, for each animal, two non-overlapping images were taken of each section at 10X magnification using the EVOS FL Auto. ImageJ was used to quantify the area of positive PSR staining above a threshold that was set based on the staining in BV-shHN treated ovary. This threshold was kept constant for all images analyzed for each ovarian section. We exclude of analysis extra-ovarian tissues as lipids and bursa that can stained red.

Cell culture

KGN cells have previously been characterized as an ovarian granulosa-like tumor cell line, from a granulosa cell tumor (Nishi *et al.* 2001). KGN cells were cultured in flasks containing DMEM: Nutrient Mixture F-12 (DMEM-F12) (GIBCO, Invitrogen) supplemented with 2.5 µg/mL amphotericin, 10 U/mL penicillin, 10 µg/mL streptomycin and 10% fetal bovine serum (FBS; Natocor, Córdoba, Argentina) at 37°C in 5% of CO_2. Then, cells were harvested with 0.025% trypsin-EDTA. KGN cells were seeded on cover slides placed in 24-well tissue culture plates (5×10^4 cells/0.5 mL/well) for immunofluorescence or TUNEL assay or in 24-well tissue culture plates (1×10^5cells/0.5 mL/well) for flow cytometry (BD FACScalibur™) analysis or Western Blot assay. For 3-(4,5-dimethylthiazol-2-yl)-2,5-diphenyltetrazolium bromide (MTT) reduction assay, KGN cells were seeded in 96-well tissue culture plates (5×10^3 cells/0.1 mL/well). Cells were cultured for 24 h in DMEM/F-12 with 10% FBS and then incubated for 24 h in DMEM/F-12 serum-free, and subsequently incubated for an additional 24 h period with HN (1 µM) in the same medium. To transduce KGN cells with recombinant baculovirus, cells were incubated for 1 h with BV-shHN (450 viral particles/cell) in DMEM/F-12 and, after addition of supplemented medium for 24 h, cells were fixed with 4% PFA for immunofluorescence and assessment of apoptosis by TUNEL.

Expression of HN measured by flow cytometry

Cultured KGN cell monolayers were harvested with 0.025% trypsin-EDTA and washed in cold PBS. After fixation with 4% PFA, cells were permeabilized with 0.1% saponin (MP Biomedicals, Solon, OH) for 10 min in the dark. Next, cells were incubated with anti-HN antibody (1:100) in PBS-0.05% saponin for 1 h at 37°C. Then, cells were washed and incubated with an anti-rabbit antibody conjugated with FITC (1:100) in PBS-0.05% saponin for another 1 h al 37°C. Finally, cells were washed, resuspended in PBS and analyzed by flow cytometry using a FACScan (Becton Dickinson, NJ, USA). Data analysis was performed using WinMDI 98 software. Nonspecific control was incubated with nonspecific IgG instead of the anti HN-specific primary antibody to determine the cut-off for HN fluorescence.

Gene transduction

Baculoviruses are enveloped DNA viruses pathogenic to invertebrates, capable of transducing different cell types such as human and murine cells, among others, without causing infection. Baculovirus were designed as previously reported (Gottardo *et al.* 2018). To detect successfully transduced cells, the construct included the coding sequence for the dTomato fluorescent reporter gene under the control of the cytomegalovirus (CMV) major immediate-early promoter in the opposite direction to the artificial gene coding for the silencing RNA construct. A recombinant AcMNPV baculovirus was produced (BV-shHN) containing the complete gene cassette described previously. A control baculovirus (BV-control) containing dTomato and no silencing gene was also constructed. Recombinant baculoviruses were propagated in an insect cell line derived from Trichoplusia ni BTI-TN-5B1-4 (High FiveTM cells; Thermo Fisher Scientific) (Gottardo *et al.* 2018). Cells were maintained in Grace's medium (Thermo Fisher Scientific) supplemented with 10% of FBS at 27°C in T-flasks until signs of infection became apparent. BVs were titrated on High Five cell monolayers as plaque forming units; these titers were coincident with infectious foci as determined in a reporter cell line expressing GFP under the control of polyhedrin (polh) promoter (Haase *et al.* 2015).

Microscopic detection of DNA fragmentation by TUNEL

Deparaffinized and rehydrated ovarian sections or KGN cells were irradiated in a microwave oven (370 W for 5 min) in

Downloaded from Bioscientifica.com at 11/28/2022 10:27:47AM
via free access

10 mM sodium citrate buffer, pH 6 and permeabilized with 0.1 % Triton X-100 in 0.1% sodium citrate for 5 min. Nonspecific labeling was prevented by incubating the preparations with blocking solution (2% blocking reagent, Roche Molecular Biochemicals GmbH,) in 150 mM NaCl and 100 mM maleic acid, pH 7.5 for 30 min at room temperature. DNA strand breaks were labeled with digoxigenin-dUTP (DIG-dUTP) using terminal deoxynucleotidyl transferase (0.18 U/µL) according to the manufacturer's protocol (Roche Molecular Biochemicals). After incubation with 10% sheep serum in PBS for 40 min, tissue sections or cells were incubated for 1 h with sheep fluorescein-conjugated anti-digoxygenin antibody (1:10) to detect the addition of DIG-dUTPs to 3'-OH ends of fragmented DNA. After incubation with DAPI for DNA staining for 10 min, they were washed with PBS, mounted with DABCO and visualized in a fluorescent light microscope (Axiophot, Carl Zeiss). Data of apoptotic cells in tissue sections were expressed as the number of TUNEL-positive cells/follicle. The percentage of KGN apoptotic cells was calculated as ((TUNEL+positive KGN cells)/total cells) × 100.

Hypodiploidy analysis by FACS

After fixation in ice-cold 70% ethanol, KGN cells were centrifuged and DNA was stained with propidium iodide (PI, 1 mg/mL) in PBS containing RNase (10 mg/mL) for 30 min at 37°C. Cells were washed, resuspended in PBS and analyzed by FACS. Fluorescence intensity of ≥20,000 gated cells/tube was analyzed using a FACScan. Cells with a PI staining intensity lower than the G0/G1 peak were considered hypodiploid. Analysis of DNA content and cell number determination were performed using WinMDI 98 software. Proportion of hypodiploid cells (Sub G0/G1) was assessed using WinMDI 98 and Cylcherd 1.2 softwares (Ferraris *et al.* 2014).

Cell viability

Cells were incubated with HN (1 µM) for 24 h. Cell viability was assessed by 3-(4,5-dimethylthiazol-2-yl)-2,5-diphenyltetrazolium bromide (MTT) reduction assay. Briefly, cells were washed in Krebs buffer and incubated for 4 h with 110 µL of a 0.5 µg/mL MTT-Krebs buffer solution. Formazan crystals obtained by MTT reduction were dissolved in 100 µL of a 0.04 N HCl-isopropanol solution. Optic densitometry (OD) was measured at 595 nm in a microplate spectrophotometer (Bio-Rad).

Western blot analysis

Total proteins from KGN cells were extracted in lysis buffer containing 250 mM NaCl, 5 mM $MgCl_2$, 50 mM NaF, 1 mM dithiothreitol (DTT), 1% IGEPAL, 0.02% sodium azide, 0.1% SD in 50 mM Tris–HCl pH 7.4 and protease inhibitor cocktail (1:100). Following centrifugation, supernatants were isolated and total proteins were quantified by the Bradford method (Bradford 1976). Samples were processed for subsequent electrophoretic separation. Forty µg of protein were mixed with loading buffer and loaded in each lane. Samples were separated by electrophoresis on 15% SDS-PAGE and transferred to a polyvinyl difluoride (PVDF) membrane. Blots were incubated overnight with mouse anti-BAX (1:20 BD Biosciences), rabbit anti-BCL2 (1:250 Santa Cruz Biotech) or rabbit anti-actin (1:4000 Sigma Chemical Co.) antibodies. This was followed by 1 h incubation with the corresponding HRP-conjugated anti-mouse or anti-rabbit secondary antibody (1:5000 Sigma Chemical Co). Immunoreactivity was detected by ECL. Images were obtained using GeneGnome XRQ NM (Syngene) and analyzed using ImageJ software package (free access). Intensity data from Bax and Bcl-2 were normalized with respect to the corresponding β-actin blot.

Statistical analysis

Data were plotted and analyzed using GraphPad Prism version 6.00 software (GraphPad Software). Results were expressed as the mean ± S.D. and evaluated using Student's *t*-test. The percentage of atretic follicles or apoptotic KGN cells were expressed as percentage of atretic follicles or TUNEL-positive cells ± 95% confidence limits (CL) of the total number of follicles or cells counted in each specific condition and evaluated by χ^2. Differences between groups were considered significant when $P<0.05$. All experiments were performed at least twice.

Results

Immunolocalization of HN in rat ovarian tissue

We first examined the presence of HN in rat ovarian tissue sections by immunohistochemistry (Fig. 1). HN was localized throughout the ovarian stromal cells,

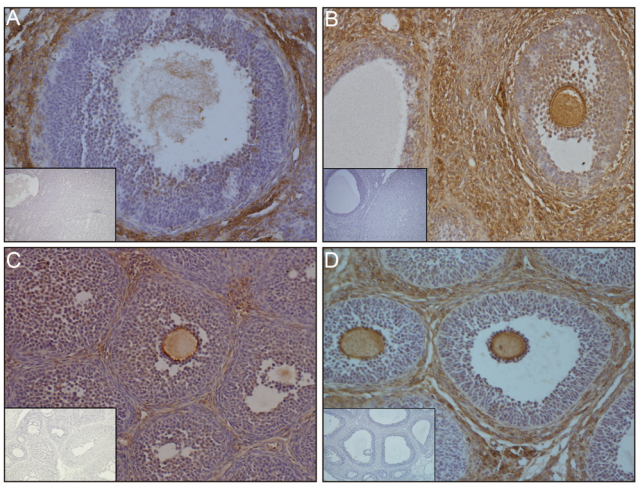

Figure 1 Immunolocalization of HN in rat ovarian tissue. Ovaries from adult Wistar cycling rats at diestrus or proestrus and prepubertal Wistar rats injected with Diethylstilbestrol (DES, enriched ovary with EAF) or Pregnant Mare Serum Gonadotropin (PMSG, enriched ovary with POF) were processed for immunohistochemistry with an anti-HN antibody followed by anti-rabbit conjugated horseradish peroxidase. The appearance of a brown reaction product indicated HN expression and the counterstaining was performed with hematoxylin. (A) Diestrus. (B) Proestrus. (C) DES. (D) PMSG. Insets show corresponding negative controls.

Downloaded from Bioscientifica.com at 11/28/2022 10:27:47AM
via free access

granulosa cells, theca cells and oocytes from adult rats at diestrus (Fig. 1A) or proestrus (Fig. 1B). However, the distribution of HN was different depending on follicular maturation stage. When follicles reach their greatest maturation as late antral follicles, we detected HN mainly in theca cells. Also, we studied HN expression in rat models of ovaries enriched with early antral follicles (EAF) or preovulatory follicles (POF), using rats treated with either diethylstilbestrol (DES) or Pregnant Mare Serum Gonadotropin (PMSG), respectively. HN staining was almost homogeneously distributed in granulosa cells, theca cells and oocytes in DES-treated rats (Fig. 1C). However, in ovaries from PMSG-treated rats (Fig. 1D), which are enriched in POF, HN staining was very low in granulosa cells and mainly detected in theca cells as we observed in late antral follicles from adult cycling rats (Fig. 1A).

Function of HN in rat ovary

To evaluate the action of endogenous HN in rat ovaries, we downregulated HN expression *in vivo*. We injected 10^7 viral particles of BV-shHN intrabursa in one ovary, and 10^7 viral particles of BV-control in the contralateral ovary (10 µL/ovary). After 14 days, ovaries were removed and processed for immunohistochemistry to determine the effect of BV-shHN. Ovaries injected with BV-control presented similar histological characteristics to untreated or PBS-treated ovaries (Fig. 2A and B). However, BV-shHN-treated ovaries revealed remarkable histological changes in respect to ovaries injected with BV-control (Fig. 2B and C). We observed that HN expression was attenuated in ovaries injected with BV-shHN in comparison with ovaries injected with BV-control (Fig. 2D and E).

We counted the number of atretic follicles (Fig. 3A and B) and we observed that the treatment with BV-shHN increased the number of atretic follicles (Fig. 3C), suggesting that HN could act as a cytoprotective factor in antral follicles. To investigate whether the inhibition of endogenous HN expression triggers apoptosis, slices of ovarian tissue from rats injected with BV-shHN were assayed by TUNEL (Fig. 3D and E). BV-shHN increased the number of apoptotic granulosa cells per antral follicle, compared with those injected with BV-control (Fig. 3F).

Considering that ovaries injected with BV-shHN change their normal histoarchitecture, we explored whether fibrosis is involved in altering the normal histology of these ovaries. To evaluate fibrosis, we detected collagen I and III by PSR staining. As expected, we detected collagen in the ovarian surface epithelium, follicles, and blood vessels (Berkholtz *et al.* 2006) in both BV-control and BV-shHN injected ovaries (Fig. 4A and B). However, in ovaries treated with BV-shHN, we observed fibrotic foci in ovarian stroma characterized by intense PSR staining (Fig. 4B). In fact, ovaries injected with BV-shHN showed a significant increase in PSR positive staining per ovarian section compared to those BV-control injected ovaries (Fig. 4C). We did not find differences in the number of atretic follicles (Fig. 5A), in the number of apoptotic granulosa cells per antral follicle (Fig. 5B) and in PSR positive staining (Fig. 5C) between PBS (vehicle) and BV-control.

Expression and function of HN in a granulosa-like tumor cell line

We explored the expression and function of HN in a granulosa-like tumor cell line (KGN).

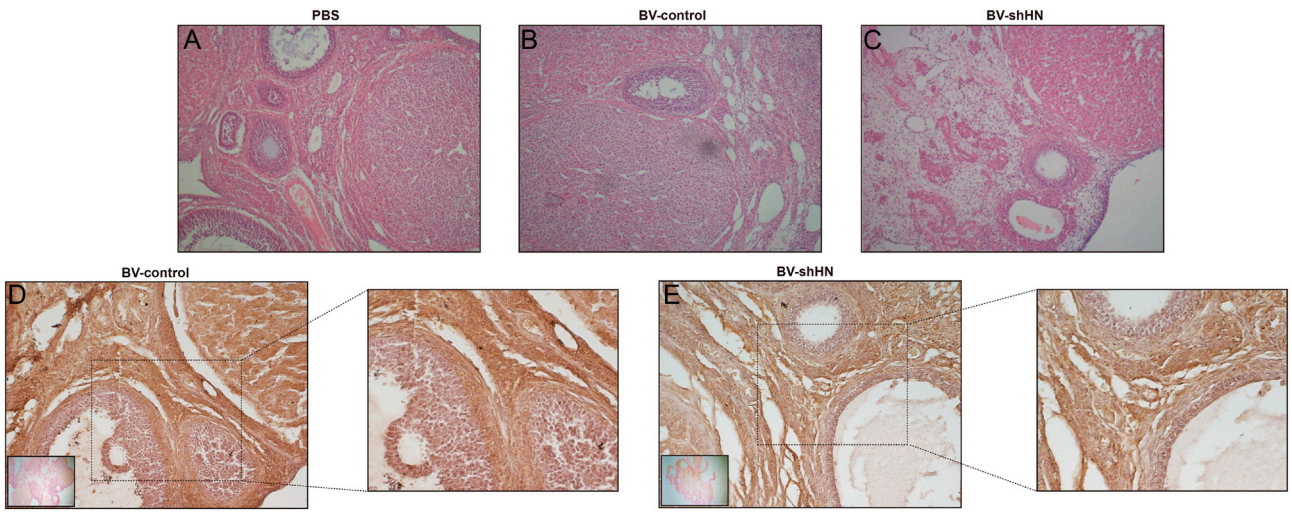

Figure 2 Downregulation of endogenous HN expression. Adult Wistar rats were injected intrabursa with PBS, BV-control or BV-shHN. Representative images of ovarian tissue injected with (A) PBS, (B) BV-control or (C) BV-shHN stained with hematoxylin-eosin. Paraffin ovary sections were processed for immunohistochemistry using an anti-HN antibody followed by anti-rabbit conjugated horseradish peroxidase. (D) BV-control, (E) BV-shHN. Insets show corresponding negative controls.

Downloaded from Bioscientifica.com at 11/28/2022 10:27:47AM
via free access

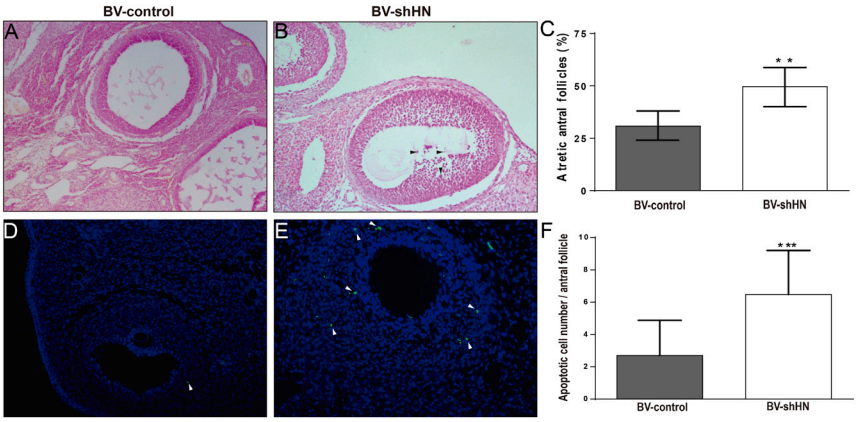

Figure 3 Effect of downregulation of endogenous HN expression. Adult Wistar rats were injected intrabursa with BV-control or BV-shHN. Representative images of ovarian tissue injected with (A) BV control or (B) BV-shHN stained with hematoxylin-eosin. Black arrows indicated pyknotic nuclei. (C) Percentage of atretic follicles (with more than 10 pyknotic nuclei) in sections from ovarian rats injected with BV-Control or BV-shHN. Each column represents the percentage ± CL of atretic follicles (3 ovarian sections per ovary) $^{**}P < 0.01$. χ^2. $n=5$. Representative fields of ovarian sections injected with (D) BV-control or (E) BV-shHN labeled by TUNEL technique. White arrows indicated representative apoptotic cells. (F) The number of apoptotic cells was determined by counting labeled cells in antral follicles. Each column represents the apoptotic granulosa cell number per follicle ± S.D. Number of analyzed follicles was between 60 and 100 follicles (three ovarian sections per ovary). $^{***}P < 0.001$. Paired Student's *t*-test. $n = 4$.

Immunofluorescence showed HN expression in the cytoplasm of KGN cells (Fig. 6A). As determined by FACS, the percentage of KGN cells expressing HN was 73% (Fig. 6B). To evaluate the role of endogenous HN in the apoptotic response of these granulosa tumor cells, we incubated them for 24 h with 450 viral particles per cell of BV-control or BV-shHN. By immunofluorescence, BV-shHN decreased HN protein expression in KGN cells compared with BV-control transduced cells (Fig. 6C).

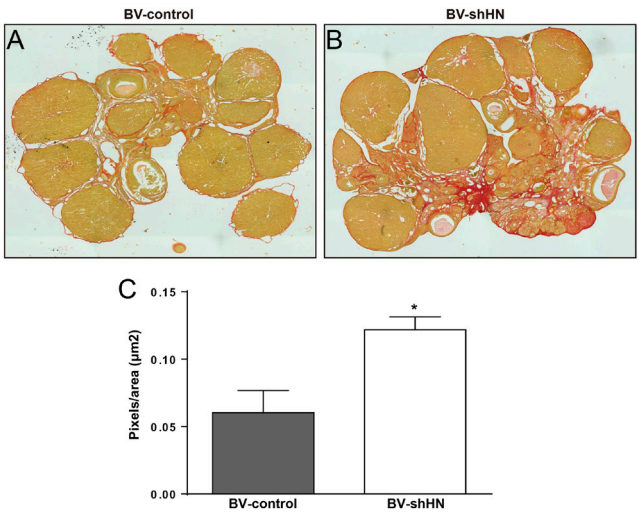

Figure 4 Effect of inhibition of endogenous HN on ovarian fibrosis. Adult Wistar rats were injected intrabursa with BV-control or BV-shHN. Representative fields of ovarian sections injected with (A) BV-control. (B) BV-shHN stained with Picrosirius red (PSR). (C) Average area of PSR-positive staining per ovarian section (pixel/µm) in BV-control and BV-shHN treated ovaries. Each column represents the mean of area/threshold ± S.E.M. (two ovarian sections per ovary). $^{*}P < 0.05$. Student's *t*-test. $n = 4$.

To evaluate the effect of downregulating HN expression on the apoptotic response of KGN cells, we determined the percentage of TUNEL-positive cells at 24 h post-transduction with BV-control or BV-shHN.

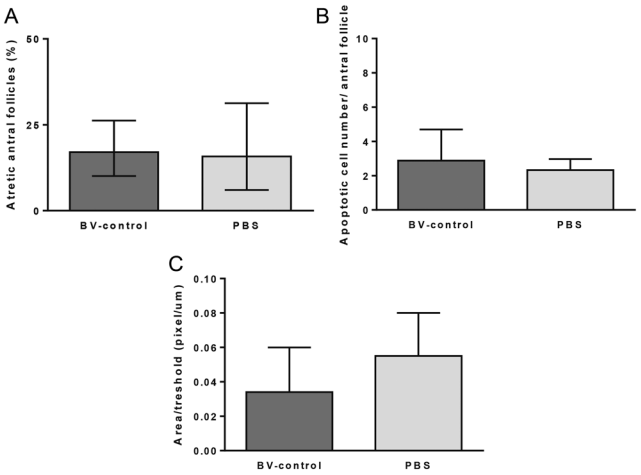

Figure 5 Effect of BV-Control or PBS on downregulation of endogenous HN expression. Adult Wistar rats were injected intrabursa with BV-Control or PBS (vehicle). (A) Percentage of atretic follicles (with more than 10 pyknotic nuclei) in sections from ovarian rats injected with BV-Control or PBS. Each column represents the percentage ± CL of atretic follicles (three ovarian sections per ovary). χ^2. $n = 2$. (B) The number of apoptotic cells was determined by counting labeled cells in antral follicles. Each column represents the apoptotic granulosa cell number per follicle ± S.E.M. Number of analyzed follicles was between 60 and 100 follicles (two ovarian sections per ovary). Paired Student's *t*-test. $n = 2$ (C) Average area of PSR-positive staining per ovarian section (pixels/µm) in BV-control and BV-shHN treated ovaries. Each column represents the mean of area/threshold ± S.E.M. (two ovarian sections per ovary). Student's *t*-test. $n = 2$.

Downloaded from Bioscientifica.com at 11/28/2022 10:27:47AM
via free access

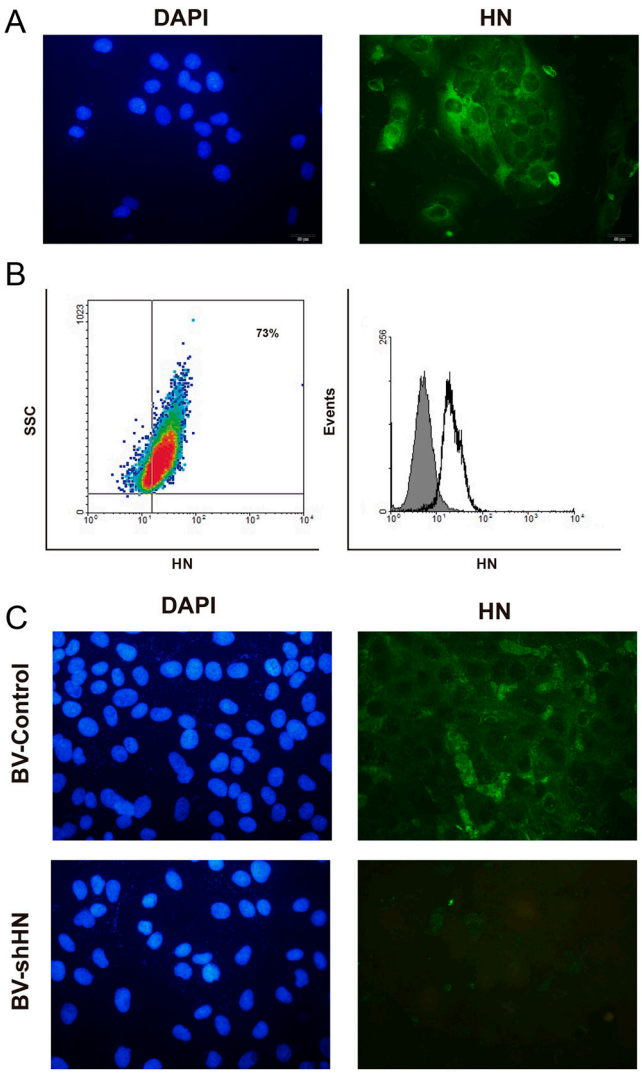

Figure 6 Expression of endogenous HN in KGN cells *in vitro*. (A) Representative images of KGN cell culture processed by immunofluorescence. Left panel: nuclear staining with DAPI. Right panel: immunocytochemistry for HN. (B) KGN cells were immunostained for HN and analyzed by flow cytometry. The graphs show representative dot plot and histograms of HN expression in KGN cells. Data from two independent experiments with five replicates were analyzed. (C) Representative images of KGN cells transduced with BV-control or BV-shHN processed for HN detection by immunofluorescence. DAPI (left panel) and HN (right panel).

BV-shHN increased apoptosis in KGN cells (Fig. 7B), suggesting that downregulation of endogenous HN expression was effective enough to trigger apoptosis in these cells.

Action of the exogenous HN on apoptosis in KGN cells

HN family peptides can be released into the extracellular space and act as cytoprotective factors in an autocrine,

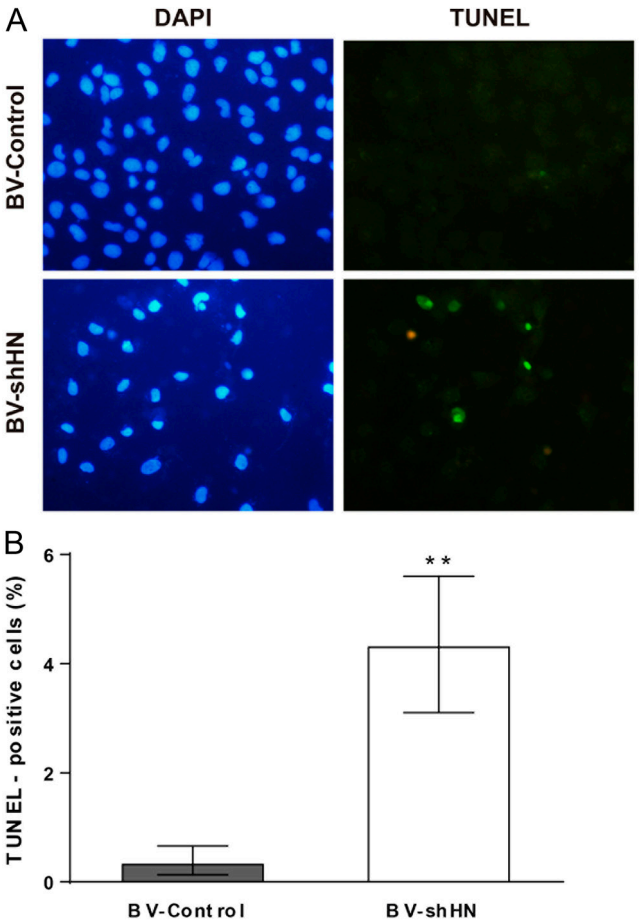

Figure 7 Function of endogenous HN in KGN cells *in vitro*. Apoptosis was evaluated by TUNEL. (A) Representative images of KGN cell culture processed by TUNEL. Left panel: nuclear staining with DAPI. Right panel: TUNEL. (B) Each column represents the percentage ± CL of TUNEL-positive KGN cells ($n \geq 1000$ cells/group). Data from three independent experiments were analyzed by χ^2 test. $^{**}P < 0.01$.

paracrine or even endocrine manner (Yen *et al.* 2013). Therefore, we explored whether exogenous HN exerts a cytoprotective effect on KGN cells. For this purpose, KGN cells were incubated with synthetic HN (1 µM) (Gottardo *et al.* 2015). We observed that HN increased cell viability (Fig. 8A). We also evaluated HN action in KGN cell death, incubating KGN cells with HN and determined the hypodiploidy and percentage of apoptotic KGN cells. HN decreased the percentage of hypodiploid KGN cells (Fig. 8B) as well as the percentage of apoptotic KGN cells (Fig. 8C). Altogether, these results suggest that HN could be considered a pro-survival factor in this tumor cell line.

In order to explore the mechanism involved in the cytoprotective action of HN, we focused on the intrinsic apoptotic pathway, especially in *Bax* and *Bcl2* expression. To study if the anti-apoptotic action of HN is through changing the protein levels of BAX and BCL2, we determined their expression in KGN cells cultured with HN by Western Blot. We showed that HN did not

Downloaded from Bioscientifica.com at 11/28/2022 10:27:47AM
via free access

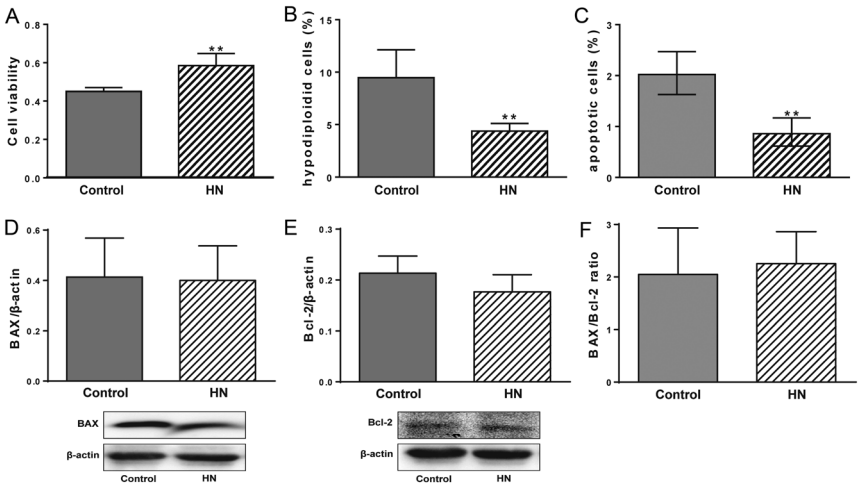

Figure 8 Action of exogenous HN on the apoptosis in KGN cells. Cell viability was assessed by (A) MTT assay measuring absorbance at 595 nm. Each column represents the mean ± S.D. of optical density of five replicates. Data from two independent experiments were analyzed by unpaired Student's *t*-test. $^{**}P < 0.01$ vs Control. Apoptosis in KGN cells was assessed by (B) Flow cytometry with IP staining. Each column represents the mean ± S.D. of percentage of hypodiploidy cells. Data from three independent experiments were analyzed by unpaired Student's *t*-test. $^{**}P < 0.01$ and (C) Nuclear staining with DAPI to detect a characteristic apoptotic morphology generated for chromatin condensation. Each column represents the percentage ± CL of apoptotic cells (n 4000–5000 cell/group). Data from three independent experiments were analyzed by χ^2 test. $^{**}P < 0.01$. (D) Proteins levels of Bax and (E) Bcl-2 measured by Western blot. Densitometric data were normalized by the corresponding β-actin value. Representative blots are shown in panel D and E, respectively. (F) BAX/Bcl-2 ratio. Each column represents the mean ± S.E.M. from three independent experiments.

modify BAX (Fig. 8D) or BCL2 (Fig. 8E) protein levels nor BAX/BCL2 ratio (Fig. 8F).

Discussion

HN has been proposed as a cytoprotective peptide in several tissues but, it is not known yet about its action in the ovary. We show that HN exerts a cytoprotective action in antral follicles, suggesting that this peptide could be involved in the follicular development and, therefore, in the physiology and tissue homeostasis of the ovary.

In our study, we localized HN in granulosa cells, oocytes and theca cells in the rat ovary which is consistent with a recent study performed in human ovary (Rao *et al.* 2018). In male rats, it was demonstrated that HN has an expression pattern and cellular localization dependent on rat testicle development, with the highest levels of HN in Leydig cells (Colón *et al.* 2006). We observed that HN presents a differential pattern distribution according to the follicular development stage, being notorious for the expression of HN in theca cells of preovulatory follicles. We hypothesize that hormones could regulate the expression of HN in follicles. In fact, we previously reported that estradiol decreases HN expression in the pituitary gland (Gottardo *et al.* 2015). As PMSG treatment of immature female rat induces a preovulatory increase in estradiol secretion and elicits a preovulatory surge of FSH/LH (Yang *et al.* 1976), it is possible that hormone fluctuation along the estrus cycle could modulate the expression and action of HN. In the present study, we showed that HN is a cytoprotective factor in granulosa cells of antral follicles. Downregulation of HN expression increased the number of pyknotic granulosa cells, which could lead to antral follicle atresia. Quality of oocytes depends on interactions with surrounding health granulosa cells. A recent report has associated oocyte quality with the number of apoptotic granulosa cells (Almeida *et al.* 2018). Since granulosa cells have a narrow interaction with the oocyte, cytoprotection of granulosa cells may impact in the oocyte's survival and so in the oogenesis. Hence, HN could be a cytoprotective factor also in the oocytes. Besides, we observed that HN is also present in oocytes so this peptide could exert its cytoprotective action in an autocrine manner too. Deregulation of HN expression could alter the dynamic of the follicles development. So HN could be involved in several ovary pathologies as PCOS, which include an excessive number of small follicles with respect to antral follicles (Dewailly *et al.* 2016). In fact, it was recently reported that HN expression was significantly downregulated in the ovaries of PCOS patients (Wang *et al.* 2021).

HN can exert its anti-apoptotic action through membrane receptors (Charununtakorn *et al.* 2016, Gottardo *et al.* 2017) and/or through an intrinsic mitochondrial mechanism by modulating the expression of proteins of the BCL2 family (Gottardo *et al.* 2017). The intrinsic mitochondrial pathway was shown to be a crucial signaling pathway for ovarian cell apoptosis (Gürsoy *et al.* 2008, Bas *et al.* 2011). In our study, we evaluated whether HN is exerting its anti-apoptotic effect through the intrinsic apoptotic pathway. Our data showed that exogenous HN does not change the BAX/

Downloaded from Bioscientifica.com at 11/28/2022 10:27:47AM
via free access

BCL2 ratio. These findings are in contrast with previous results from our group where HN decreased BAX/BCL2 ratio in a pituitary tumor cell line (Gottardo *et al.* 2017). However, it is known that modifications in Bcl-2 family proteins are tissue specific (Yuan *et al.* 2020). Also, HN can heterodimerize with BAX and prevents its translocation to the mitochondria and therefore its depolarization and the release of cytochrome c (Ma & Liu 2018, Morris *et al.* 2019). Thus, although our results demonstrate that HN exerts a pro-survival role in granulosa cells, further studies are required to determine its precise mechanism of action.

Several studies have shown that HN content in plasma decreases with age (Bachar *et al.* 2010) and that there is a significant loss of HN in skeletal muscle of rats with aging (Muzumdar *et al.* 2009). In our study, the inhibition of endogenous HN modified the histoarchitecture of the ovary, which showed a thinner cortex and a disorganized medulla, changes that are similar to those observed in the aged ovary (Laszczyńska *et al.* 2008). Fibrosis increases in the ovary with advanced reproductive age due to increased synthesis and deposition and/or altered post-translational modifications of collagen or other extracellular matrix components (Briley *et al.* 2016). Here, we show that the inhibition of endogenous HN increases collagen within the ovary. This result suggests that HN could be involved in the maintenance of a normal extracellular matrix to generate an adequate ovarian environment, supporting the idea that HN could act as an anti-aging peptide in the ovary. How and by what pathway HN exerts its action in this process still needs further investigation.

Other changes in the ovarian tissue characteristic of aging are associated with a reduction in the number of follicles due to apoptotic processes (Laszczyńska *et al.* 2008). In our study, we observed that HN exerts a relevant anti-apoptotic action in granulosa cells of antral follicles. Therefore, HN could be also considered as an anti-aging factor in the ovary, maintaining the viability and therefore the number of follicles.

HN was reported to be overexpressed in gastric and pituitary cancer cells, where this peptide exerted anti-apoptotic action, suggesting that HN overexpression could be an important molecular event in tumor behavior. Our results showed that HN is present in KGN cells and exerts an anti-apoptotic effect on these tumor cells. We think that HN could be an interesting target peptide to study in the pathogenesis and behavior of granulosa tumors. As Gottardo *et al.* proposed (Gottardo *et al.* 2018), our results also suggest the BVs as a promising tool for clinical trials. Lack of toxicity and replication, as well as the absence of pre-existing immunity in mammalian hosts, make BVs very attractive vectors for gene therapy applications.

In conclusion, our findings provide evidence that HN is expressed in the rat ovary and that it is implicated in the survival of antral follicles, preventing apoptosis of granulosa cells and therefore modulating follicular atresia. Also, we show that HN is involved in the conservation of ovarian histoarchitecture (Mottaghi-Dastjerdi *et al.* 2014, Gottardo *et al.* 2015. Taken together, our study suggests that HN is a cytoprotective factor and that could contribute to physiological homeostasis in the ovary. On the other hand, HN is also expressed in tumoral granulosa cells and behaves as an anti-apoptotic factor, whereby could be a promissory target to study in tumoral granulosa cells.

Declaration of interest

The authors declare that there is no conflict of interest that could be perceived as prejudicing the impartiality of the research reported.

Funding

This work was partially supported by grants from the National Agency of Scientific and Technologic Promotion (PICT 2014-0334 and PICT 2016-0519) and the University of Buenos Aires (UBACyT 20020130100020BA and 20020170100343BA).

Author contribution statement

C M performed the experiments, statistical analysis and wrote the first draft of the manuscript. D M and M I performed immunohistochemistry and TUNEL techniques. J G C performed KGN culture to determine Bax and Bcl2 expression. G J designed the experiments, discussed results and revised the first draft of the manuscript. M F G and M L P designed baculovirus and produced it. S L M and F E D performed picrosirius red staining and read and edited the manuscript. M Imsen collaborated with animal handling and performing the anesthesia procedures. G J, V R, A S and F E D reviewed the manuscript and approved the submitted version.

Acknowledgements

The authors thank Cecilia García for her technical assistance with histological procedures. The authors also thank to Ana Clara Romero for her excellent technical support in the cell culture lab.

References

Agarwal A, Aponte-Mellado A, Premkumar BJ, Shaman A & Gupta S 2012 The effects of oxidative stress on female reproduction: a review. *Reproductive Biology and Endocrinology* **10** 49. (https://doi.org/10.1186/1477-7827-10-49)

Almeida CP, Ferreira MCF, Silveira CO, Campos JR, Borges IT, Baeta PG, Silva FHS, Reis FM & Del Puerto HL 2018 Clinical correlation of apoptosis in human granulosa cells – a review. *Cell Biology International* **42** 1276–1281. (https://doi.org/10.1002/cbin.11036)

Bachar AR, Scheffer L, Schroeder AS, Nakamura HK, Cobb LJ, Oh YK, Lerman LO, Pagano RE, Cohen P & Lerman A 2010 Humanin is expressed in human vascular walls and has a cytoprotective effect against oxidized LDL-induced oxidative stress. *Cardiovascular Research* **88** 360–366. (https://doi.org/10.1093/cvr/cvq191)

Downloaded from Bioscientifica.com at 11/28/2022 10:27:47AM
via free access

Bas D, Abramovich D, Hernandez F & Tesone M 2011 Altered expression of Bcl-2 and Bax in follicles within dehydroepiandrosterone-induced polycystic ovaries in rats. *Cell Biology International* **35** 423–429. (https://doi.org/10.1042/CBI20100542)

Berkholtz CB, Lai BE, Woodruff TK & Shea LD 2006 Distribution of extracellular matrix proteins type I collagen, type IV collagen, fibronectin, and laminin in mouse folliculogenesis. *Histochemistry and Cell Biology* **126** 583–592. (https://doi.org/10.1007/s00418-006-0194-1)

Bradford MM 1976 A rapid and sensitive method for the quantitation of microgram quantities of protein utilizing the principle of protein-dye binding. *Analytical Biochemistry* **72** 248–254. (https://doi.org/10.1016/0003-2697(76)90527-3)

Briley SM, Jasti S, McCracken JM, Hornick JE, Fegley B, Pritchard MT & Duncan FE 2016 Reproductive age-associated fibrosis in the stroma of the mammalian ovary. *Reproduction* **152** 245–260. (https://doi.org/10.1530/REP-16-0129)

Caricasole A, Bruno V, Cappuccio I, Melchiorri D, Copani A & Nicoletti F 2002 A novel rat gene encoding a humanin-like peptide endowed with broad neuroprotective activity. *FASEB Journal* **16** 1331–1333. (https://doi.org/10.1096/fj.02-0018fje)

Charununtakorn ST, Shinlapawittayatorn K, Chattipakorn SC & Chattipakorn N 2016 Potential roles of humanin on apoptosis in the heart. *Cardiovascular Therapeutics* **34** 107–114. (https://doi.org/10.1111/1755-5922.12168)

Colón E, Strand ML, Carlsson-Skwirut C, Wahlgren A, Svechnikov KV, Cohen P & Söder O 2006 Anti-apoptotic factor humanin is expressed in the testis and prevents cell-death in Leydig cells during the first wave of spermatogenesis. *Journal of Cellular Physiology* **208** 373–385. (https://doi.org/10.1002/jcp.20672)

Dewailly D, Robin G, Peigne M, Decanter C, Pigny P & Catteau-Jonard S 2016 Interactions between androgens, FSH, anti-Mullerian hormone and estradiol during folliculogenesis in the human normal and polycystic ovary. *Human Reproduction Update* **22** 709–724. (https://doi.org/10.1093/humupd/dmw027)

Ferraris J, Zárate S, Jaita G, Boutillon F, Bernadet M, Auffret J, Seilicovich A, Binart N, Goffin V & Pisera D 2014 Prolactin induces apoptosis of lactotropes in female rodents. *PLoS ONE* **9** e97383. (https://doi.org/10.1371/journal.pone.0097383)

Gottardo MF, Jaita G, Magri ML, Zárate S, Moreno Ayala MM, Ferraris J, Eijo G, Pisera D, Candolfi M & Seilicovich A 2015 Correction: Antiapoptotic factor humanin is expressed in normal and tumoral pituitary cells and protects them from TNF-α-induced apoptosis. *PLoS ONE* **10** 1–4. (https://doi.org/10.1371/journal.pone.0124589)

Gottardo MF, Moreno Ayala M, Ferraris J, Zárate S, Pisera D, Candolfi M, Jaita G & Seilicovich A 2017 Humanin inhibits apoptosis in pituitary tumor cells through several signaling pathways including NF-κB activation. *Journal of Cell Communication and Signaling* **11** 329–340. (https://doi.org/10.1007/s12079-017-0388-4)

Gottardo MF, Pidre ML, Zuccato C, Asad AS, Imsen M, Jaita G, Candolfi M, Romanowski V & Seilicovich A 2018 Baculovirus-based gene silencing of humanin for the treatment of pituitary tumors. *Apoptosis* **23** 143–151. (https://doi.org/10.1007/s10495-018-1444-0)

Gürsoy E, Ergin K, Başaloğlu H, Koca Y & Seyrek K 2008 Expression and localisation of Bcl-2 and Bax proteins in developing rat ovary. *Research in Veterinary Science* **84** 56–61. (https://doi.org/10.1016/j.rvsc.2007.04.006)

Haase S, López MG, Taboga O & Romanowski V 2015 Reporter high FiveTM XXL-GFP cell line induced by AcMNPV-DsRED baculovirus infection (clinical image). *Cloning Transgenes* **4** i102. (https://doi.org/10.4172/2168-9849.1000i102)

Hashimoto Y, Ito Y, Niikura T, Shao Z, Hata M, Oyama F & Nishimoto I 2001*a* Mechanisms of neuroprotection by a novel rescue factor humanin from Swedish mutant amyloid precursor protein. *Biochemical and Biophysical Research Communications* **283** 460–468. (https://doi.org/10.1006/bbrc.2001.4765)

Hashimoto Y, Niikura T, Ito Y, Sudo H, Hata M, Arakawa E, Abe Y, Kita Y & Nishimoto I 2001*b* Detailed characterization of neuroprotection by a rescue factor humanin against various Alzheimer's disease-relevant insults. *Journal of Neuroscience* **21** 9235–9245. (https://doi.org/10.1523/jneurosci.21-23-09235.2001)

Hashimoto Y, Terashita K, Niikura T, Yamagishi Y, Ishizaka M, Kanekura K, Chiba T, Yamada M, Kita Y, Aiso S *et al.* 2004 Humanin antagonists: mutants that interfere with dimerization inhibit neuroprotection by humanin. *European Journal of Neuroscience* **19** 2356–2364. (https://doi.org/10.1111/j.0953-816X.2004.03298.x)

Hsueh AJW, Billig H & Tsafriri A 1994 Ovarian follicle atresia: a hormonally controlled apoptotic process. *Endocrine Reviews* **15** 707–724. (https://doi.org/10.1210/edrv-15-6-707)

Kariya S, Hirano M, Furiya Y, Sugie K & Ueno S 2005 Humanin detected in skeletal muscles of MELAS patients: a possible new therapeutic agent. *Acta Neuropathologica* **109** 367–372. (https://doi.org/10.1007/s00401-004-0965-5)

Laszczyńska M, Brodowska A, Starczewski A, Masiuk M & Brodowski J 2008 Human postmenopausal ovary – hormonally inactive fibrous connective tissue or more? *Histology and Histopathology* **23** 219–226. (https://doi.org/10.14670/HH-23.219)

Li J, Kim JM, Liston P, Li M, Miyazaki T, Mackenzie AE, Korneluk RG & Tsang BK 1998 Expression of inhibitor of apoptosis proteins (IAPs) in rat granulosa cells during ovarian follicular development and atresia. *Endocrinology* **139** 1321–1328. (https://doi.org/10.1210/endo.139.3.5850)

Lim J & Luderer U 2011 Oxidative damage increases and antioxidant gene expression decreases with aging in the mouse ovary. *Biology of Reproduction* **84** 775–782. (https://doi.org/10.1095/biolreprod.110.088583)

Lim J, Nakamura BN, Mohar I, Kavanagh TJ & Luderer U 2015 Glutamate cysteine ligase modifier subunit (Gclm) null mice have increased ovarian oxidative stress and accelerated age-related ovarian failure. *Endocrinology* **156** 3329–3343. (https://doi.org/10.1210/en.2015-1206)

Lue Y, Swerdloff R, Liu Q, Mehta H, Hikim AS, Lee KW, Jia Y, Hwang D, Cobb LJ, Cohen P *et al.* 2010 Opposing roles of insulin-like growth factor binding protein 3 and humanin in the regulation of testicular germ cell apoptosis. *Endocrinology* **151** 350–357. (https://doi.org/10.1210/en.2009-0577)

Ma ZW & Liu DX 2018 Humanin decreases mitochondrial membrane permeability by inhibiting the membrane association and oligomerization of Bax and Bid proteins. *Acta Pharmacologica Sinica* **39** 1012–1021. (https://doi.org/10.1038/aps.2017.169)

Moretti E, Giannerini V, Rossini L, Matsuoka M, Trabalzini L & Collodel G 2010 Immunolocalization of humanin in human sperm and testis. *Fertility and Sterility* **94** 2888–2890. (https://doi.org/10.1016/j.fertnstert.2010.04.075)

Morris DL, Kastner DW, Johnson S, Strub MP, He Y, Bleck CKE, Lee DY & Tjandra N 2019 Humanin induces conformational changes in the apoptosis regulator BAX and sequesters it into fibers, preventing mitochondrial outer-membrane permeabilization. *Journal of Biological Chemistry* **294** 19055–19065. (https://doi.org/10.1074/jbc.RA119.011297)

Mottaghi-Dastjerdi N, Soltany-Rezaee-Rad M, Sepehrizadeh Z, Roshandel G, Ebrahimifard F & Setayesh N 2014 Genome expression analysis by suppression subtractive hybridization identified overexpression of humanin, a target gene in gastric cancer chemoresistance. *DARU: Journal of Pharmaceutical Sciences* **22** 1–7. (https://doi.org/10.1186/2008-2231-22-14)

Muzumdar RH, Huffman DM, Atzmon G, Buettner C, Cobb LJ, Fishman S, Budagov T, Cui L, Einstein FH, Poduval A *et al.* 2009 Humanin: a novel central regulator of peripheral insulin action. *PLoS ONE* **4** e6334. (https://doi.org/10.1371/journal.pone.0006334)

Nishi Y, Yanase T, Mu YM, Oba K, Ichino I, Saito M, Nomura M, Mukasa C, Okabe T, Goto K *et al.* 2001 Establishment and characterization of a steroidogenic human granulosa-like tumor cell line, KGN, that expresses functional follicle-stimulatinghormone receptor. *Endocrinology* **142** 437–445. (https://doi.org/10.1210/endo.142.1.7862)

Nishimoto I, Matsuoka M & Niikura T 2004 Unravelling the role of humanin. *Trends in Molecular Medicine* **10** 102–105. (https://doi.org/10.1016/j.molmed.2004.01.001)

Paharkova V, Alvarez G, Nakamura H, Cohen P & Lee KW 2015 Rat humanin is encoded and translated in mitochondria and is localized to the mitochondrial compartment where it regulates ROS production. *Molecular and Cellular Endocrinology* **413** 96–100. (https://doi.org/10.1016/j.mce.2015.06.015)

Parborell F, Abramovich D & Tesone M 2008 Intrabursal administration of the antiangiopoietin 1 antibody produces a delay in rat follicular

Downloaded from Bioscientifica.com at 11/28/2022 10:27:47AM
via free access

development associated with an increase in ovarian apoptosis mediated by changes in the expression of BCL2 related genes. *Biology of Reproduction* **78** 506–513. (https://doi.org/10.1095/biolreprod.107.063610)

Rao M, Zhou F, Tang L, Zeng Z, Hu S, Wang Y, Ke D, Cheng G, Xia W, Zhang L *et al.* 2018 Follicular fluid humanin concentration is related to ovarian reserve markers and clinical pregnancy after IVF–ICSI: a pilot study. *Reproductive Biomedicine Online* **38** 108–117. (https://doi.org/10.1016/j.rbmo.2018.11.002)

Rodgers RJ & Irving-Rodgers HF 2010 Formation of the ovarian follicular antrum and follicular fluid. *Biology of Reproduction* **82** 1021–1029. (https://doi.org/10.1095/biolreprod.109.082941)

Tilly JL, Tilly KI, Kenton ML & Johnson AL 1995 Expression of members of the bcl-2 gene family in the immature rat ovary: equine chorionic gonadotropin-mediated inhibition of granulosa cell apoptosis is associated with decreased bax and constitutive bcl-2 and bcl-xlong messenger ribonucleic acid levels. *Endocrinology* **136** 232–241. (https://doi.org/10.1210/endo.136.1.7828536)

Wang Y, Li N, Zeng Z, Tang L, Zhao S, Zhou F, Zhou L, Xia W, Zhu C & Rao M 2021 Humanin regulates oxidative stress in the ovaries of polycystic ovary syndrome patients via the Keap1/Nrf2 pathway. *Molecular Human Reproduction* **27** gaaa081. (https://doi.org/10.1093/molehr/gaaa081)

Widmer RJ, Flammer AJ, Herrmann J, Rodriguez-Porcel M, Wan J, Cohen P, Lerman LO & Lerman A 2013 Circulating humanin levels are associated with preserved coronary endothelial function. *American Journal of Physiology: Heart and Circulatory Physiology* **304** H393–H397. (https://doi.org/10.1152/ajpheart.00765.2012)

Woodruff TK, Lyon RJ, Hansen SE, Rice GC & Mather JP 1990 Inhibin and activin locally regulate rat ovarian folliculogenesis. *Endocrinology* **127** 3196–3205. (https://doi.org/10.1210/endo-127-6-3196)

Yadav VK, Muraly P & Medhamurthy R 2004 Identification of novel genes regulated by LH in the primate corpus luteum: insight into their regulation during the late luteal phase. *Molecular Human Reproduction* **10** 629–639. (https://doi.org/10.1093/molehr/gah089)

Yang KP, Samaan NA & Ward DN 1976 Characterization of an inhibitor for luteinizing hormone receptor site binding. *Endocrinology* **98** 233–241. (https://doi.org/10.1210/endo-98-1-233)

Yen K, Lee C, Mehta H & Cohen P 2013 The emerging role of the mitochondrial-derived peptide humanin in stress resistance. *Journal of Molecular Endocrinology* **50** R11–R19. (https://doi.org/10.1530/JME-12-0203)

Young JM & McNeilly AS 2010 Theca: the forgotten cell of the ovarian follicle. *Reproduction* **140** 489–504. (https://doi.org/10.1530/REP-10-0094)

Yuan J, Lan H, Jiang X, Zeng D & Xiao S 2020 Bcl-2 family: novel insight into individualized therapy for ovarian cancer (Review). *International Journal of Molecular Medicine* **46** 1255–1265. (https://doi.org/10.3892/ijmm.2020.4689)

Zapała B, Kaczyński Ł, Kieć-Wilk B, Staszel T, Knapp A, Thoresen GH, Wybrańska I & Dembińska-Kieć A 2010 Humanins, the neuroprotective and cytoprotective peptides with antiapoptotic and anti-inflammatory properties. *Pharmacological Reports* **62** 767–777. (doi:10.1016/S1734-1140(10)70337-6)

Zuccato CF, Asad AS, Nicola Candia AJ, Gottardo MF, Moreno Ayala MA, Theas MS, Seilicovich A & Candolfi M 2018 Mitochondrial-derived peptide humanin as therapeutic target in cancer and degenerative diseases. *Expert Opinion on Therapeutic Targets* **23** 117–126. (https://doi.org/10.1080/14728222.2019.1559300)

Received 8 April 2020
First decision 27 May 2020
Revised Manuscript received 15 March 2021
Accepted 25 March 2021

Downloaded from Bioscientifica.com at 11/28/2022 10:27:47AM
via free access